Stimulation of Topoisomerase II-Mediated DNA Cleavage by Three DNA-Intercalating Plant Alkaloids: Cryptolepine, Matadine, and Serpentine[†]

Laurent Dassonneville,[‡] Karine Bonjean,[§] Marie-Claire De Pauw-Gillet,[§] Pierre Colson,[||] Claude Houssier,[||] Joëlle Quetin-Leclercq,[⊥,@] Luc Angenot,[⊥] and Christian Bailly*[,‡]

INSERM U524 and Laboratoire de Pharmacologie Antitumorale du Centre Oscar Lambret, IRCL, Place de Verdun, 59045 Lille, France, and Laboratoire d'Histologie et de Cytologie, Institut d'Anatomie, Université de Liège, Rue de Pitteurs, 20, 4020 Liège, Laboratoire de Chimie Macromoléculaire et Chimie Physique, Institut de Chimie, Université de Liège, Sart-Tilman, 4000 Liège, and Laboratoire de Pharmacognosie and Institut de Pharmacie, Université de Liège, CHU, Tour 4, Avenue de l'Hôpital, 4000 Liège, Belgium

Received January 15, 1999; Revised Manuscript Received April 8, 1999

ABSTRACT: Cryptolepine, matadine, and serpentine are three indoloquinoline alkaloids isolated from the roots of African plants: *Cryptolepis sanguinolenta*, *Strychnos gossweileri*, and *Rauwolfia serpentina*, respectively. For a long time, these alkaloids have been used in African folk medicine in the form of plant extracts for the treatment of multiple diseases, in particular as antimalarial drugs. To date, the molecular basis for their diverse biological effects remains poorly understood. To elucidate their mechanism of action, we studied their interaction with DNA and their effects on topoisomerase II. The strength and mode of binding to DNA of the three alkaloids were investigated by spectroscopy. The alkaloids bind tightly to DNA and behave as typical intercalating agents. All three compounds stabilize the topoisomerase II−DNA covalent complex and stimulate the cutting of DNA by topoisomerase II. The poisoning effect is more pronounced with cryptolepine than with matadine and serpentine, but none of the drugs exhibit a preference for cutting at a specific base. Cryptolepine which binds 10-fold more tightly to DNA than the two related alkaloids proves to be much more cytotoxic toward B16 melanoma cells than matadine and serpentine. The cellular consequences of the inhibition of topoisomerase II by cryptolepine were investigated using the HL60 leukemia cell line. The flow cytometry analysis shows that the drug alters the cell cycle distribution, but no sign of drug-induced apoptosis was detected when evaluating the internucleosomal fragmentation of DNA in cells. Cryptolepine-treated cells probably die via necrosis rather than via apoptosis. The results provide evidence that DNA and topoisomerase II are the primary targets of cryptolepine, matadine, and serpentine.

For almost thirty years, the "War on Cancer" has consumed the dedicated efforts of innumerable scientists throughout the world. Undeniable progress has been made to improve treatments of human cancer. At present, childhood leukemia, Hodgkin's disease, and other forms of cancer are relatively well-treated, but in contrast, there has been limited advances in the treatment of metastatic diseases such as those arising from lung and colon cancers. Efficacious drugs and regimen are still eagerly awaited.

Natural products represent a rich and largely untapped resource for the discovery of drugs with potential application for the treatment of contemporary diseases that inflict humans (*1*). This is particularly apropos to cancer treatment. For more than half a century, cancer chemotherapy has relied largely on the use of natural products such as antibiotics produced by Streptomycetes (e.g., bleomycin, actinomycin, and daunomycin) and plant-derived drugs such as etoposide, vincristine, and the related semisynthetic alkaloid vinorelbine, to cite only a few of them. The anticancer agents paclitaxel and topotecan, both recently introduced in the clinic, are also present in terrestrial plants. Plants and plant-derived drugs play a dominant role in contemporary chemotherapy of cancer as well as many other diseases (*1*).

Straightforward procedures for isolation from plant extracts have led to and no doubt will continue to lead to the discovery of valuable therapeutic agents. Once a novel promising leading prototype has been identified and its mechanism of action (or molecular recognition sites) characterized, at least partially, then chemists can envisage the structure−activity relationships via the development of more active and less toxic analogues of the leader compound. In this study, we have investigated the interaction of three rare

[†] This work was supported by research grants from the Ligue Nationale Française Contre le Cancer (to C.B.) and from the Actions de Recherches Concertées (Grant 95/00-193 to C.H. and P.C.). Support by the "convention INSERM-CFB" is acknowledged, from Fonds Spéciaux pour la Recherche dans les Universités (to L.A.). L.D. is currently supported by a fellowship from the Institut de Recherches sur le Cancer de Lille and the Conseil Régional de la Région Nord-Pas de Calais.

* Corresponding author. Fax: (+33) 320 16 92 29. E-mail: bailly@lille.inserm.fr.

[‡] INSERM U524.

[§] Institut d'Anatomie, Université de Liège.

[||] Institut de Chimie, Université de Liège.

[⊥] Laboratoire de Pharmacognosie and Institut de Pharmacie, Université de Liège.

[@] Present address: Laboratoire de Pharmacognosie, Université Catholique de Louvain, 1200 Bruxelles, Belgium.

10.1021/bi990094t CCC: $18.00
Published on Web 05/26/1999

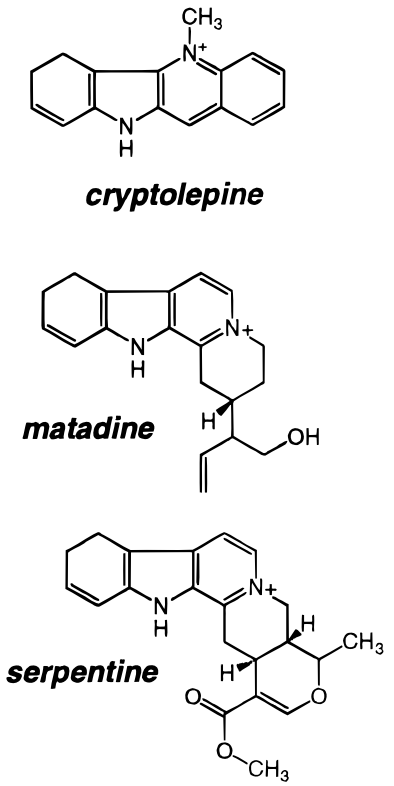

FIGURE 1: Structure of the alkaloids.

plant alkaloids—cryptolepine, matadine, and serpentine (Figure 1)—with their molecular targets.

Cryptolepine was first isolated in 1929 from the roots of the African plant *Cryptolepis triangularis* found in Kisantu (Zaïre), and later this indoloquinoline alkaloid was also extracted from *Cryptolepis sanguinolenta* from Nigeria (*2*, *3*). Cryptolepine possesses numerous biological properties, including anti-hyperglycemic and antimalarial activities (*3*−*6*). Extracts of the roots of *C. sanguinolenta* are still used clinically in Ghana for the treatment of malaria (*7*), but cryptolepine itself is only weakly active in vivo against *Plasmodium berghei berghei* (*8*). Extracts from *Cryptolepis* plants have also been used in African folk medicine as a remedy against colic and as a stomach tonic. In addition, cryptolepine is a cytotoxic agent inhibiting DNA synthesis in B16 melanoma cells (*9*).

Matadine, isolated from the root bark of *Strychnos gossweileri*, bears a structural analogy to cryptolepine (Figure 1). The name matadine was chosen because the plant *S. gossweileri* was collected in Matadi (Zaïre). Very little is known concerning its mechanism of action, but it is interesting to note that matadine is more toxic to B16 melanoma and HeLa carcinoma cells than to noncancerous mouse 3T3 fibroblasts and human 2002 cells (*10*).

Serpentine was isolated from *Rauwolfia serpentina* but is also present in Apocynaceae and in *Strychnos camptoneura*. It is an isomer of the drug called alstonine. The bark of several species of *Alstonia* are used widely in Asia as well as in West Africa for the treatment of malaria (*11*). Serpentine itself has moderate antitumor activities (*12*, *13*).

In a recent study, we showed that cryptolepine behaves as a typical DNA-intercalating agent and we presented preliminary results suggesting that the drug can interfere with topoisomerase II (*14*). We have now extended our study to compare the three aforementioned anhydronium alkaloids: cryptolepine, matadine, and serpentine.

MATERIALS AND METHODS

Drugs. The three alkaloids were isolated and purified as previously described (*8*, *10*). They were initially dissolved in methanol (at a concentration of 10 mM) prior to dilution with water.

Chemicals and Biochemicals. Calf thymus DNA (Sigma Chemical Co., La Verpillière, France) was deproteinized with sodium dodecyl sulfate and dialyzed against 1 mM sodium cacodylate-buffered solution (pH 6.5). [γ-^{32}P]ATP was obtained from Amersham (Buckinghamshire, England). Restriction endonucleases *Ava*I, *Eco*RI, *Hin*dIII, and *Pvu*II, alkaline phosphatase, T4 polynucleotide kinase, and AMV reverse transcriptase were purchased from Boehringer (Mannheim, Germany).

Absorption Spectroscopy. Absorption spectra were recorded on a Perkin-Elmer Lambda 5 spectrophotometer using a 10 mm optical path length. Titrations of the drug with DNA were performed by adding aliquots of a concentrated DNA solution to a drug solution at constant ligand concentration (20 μM). Binding constants were determined using experimental spectrophotometric readings from absorbance titration experiments conducted at 367 nm.

Fluorescence polarization measurements were expressed as anisotropy values *r*,

$$r = [1 - N(I_{VV}/I_{VH})]/[2 + N(I_{VV}/I_{VH})]$$

where *N* is the correction factor for the transmittivity of the emission monochromator, were taken on a Perkin-Elmer LS 50 spectrofluorimeter. Fluorescence emission spectra were measured from 480 to 620 nm with an excitation wavelength of 426 nm.

Electric linear dichroism (ELD) measurements were taken with a computerized optical measurement system (*15*) using the procedures previously outlined (*16*). All experiments were conducted with a 10 mm path length Kerr cell having a 1.5 mm electrode separation. The samples were oriented under an electric field strength varying from 1 to 13 kV/cm. The reduced dichroism $\Delta A/A = (A_{||} - A_{\perp})/A$, where A is the isotropic absorbance of the sample measured in the absence of field at the same wavelength and under the same path length (10 nm). $A_{||}$ and $A_{\perp}$ are the absorbances of light polarized parallel and perpendicular to the electric field vector, respectively. This electro-optical method has proven to be most useful as a means of determining the orientation of the drugs bound to DNA, and has the additional advantage that it senses only the orientation of the polymer-bound ligand; free ligand is isotropic and does not contribute to the signal (*17*, *18*).

DNA Purification and Labeling. The two pBS DNA fragments were prepared by 5′-^{32}P-end labeling of the *Eco*RI/alkaline phosphatase-treated plasmid using [γ-^{32}P]ATP and T4 polynucleotide kinase followed by treatment with *Pvu*II. Similarly, the 155-mer and 178-mer fragments were prepared by 3′-end labeling of the *Eco*RI−*Hin*dIII and *Eco*RI−*Pvu*II digests, respectively, of plasmid pLAZ3 (*19*).

Topoisomerase II DNA Cleavage Reaction. The cleavage reaction mixture contained 20 mM Tris-HCl (pH 7.4), 60 mM KCl, 0.5 mM EDTA, 0.5 mM dithiothreitol, 10 mM

$MgCl_2$, 1 mM ATP, 500 cpm of [γ-^{32}P]pBS DNA, and the indicated drug concentrations. The reaction was initiated by the addition of human topoisomerase II (10 units, p170 form from TopoGen Inc., Columbus, OH) and allowed to proceed for 30 min at 37 °C. Reactions were stopped by adding SDS to a final concentration of 0.25% and proteinase K to 250 μg/mL, followed by incubation for 30 min at 50 °C. Five microliters of loading buffer [30 mM EDTA, 15% (w/v) sucrose, and 0.1% electrophoresis dye] was added to each sample prior to loading onto a 1% agarose gel in TBE-buffered solution containing 0.1% SDS. DNA cleavage products were resolved by polyacrylamide gel electrophoresis under denaturing conditions (8% acrylamide and 8 M urea). After electrophoresis, gels were soaked in 10% acetic acid for 10 min, transferred to Whatman 3MM paper, and dried under vacuum at 80 °C. A Molecular Dynamics 425E PhosphorImager was used to collect and analyze the data.

Immunoblot Assay of Topoisomerase II−DNA Complexes in Cells. The in vivo topoisomerase II link kit of TopoGEN, Inc., was used. Briefly, 10^7 exponentially growing HL60 cells in 5 mL of serum-free RPMI 1640 medium were treated with the test drug at a concentration of 50 μM for 30 min at 37 °C. Cells were pelleted by centrifugation (1000 rpm for 5 min) and rapidly resuspended in 0.8 mL of the lysis buffer [10 mM Tris-HCl (pH 7.5), 1 mM EDTA, and 1% sarkosyl]. The lysed cell mixture was then overlaid onto a CsCl density gradient containing four different density steps (0.8 mL of CsCl at 1.82, 1.72, 1.50, and 1.37 g/mL). The tubes were centrifuged in a Beckman SW60 rotor at 31 000 rpm (13000*g*) for 15 h at 25 °C. From the top of the gradient, 12 fractions of 330 μL were collected. The DNA content in each fraction was estimated by absorbance measurement at 260 nm. For the immunoblot analysis, 50 μL of each fraction was diluted with 100 μL of 25 mM sodium phosphate buffer (PBS, pH 6.5) prior to applying the diluted solution into the slot blot unit under a mild vacuum. PBS-washed Hybond-C nitrocellulose membranes (Amersham) cut to fit the vacuum slot blot device (Life Science, Cergy-Pontoise, France) were loaded with the diluted samples, and the samples were washed briefly with PBS and then soaked for 2 h in TBSTB [20 mM Tris-HCl (pH 7.6), 137 mM NaCl, 0.1% Tween 20, and 1% bovine serum albumin] supplemented with 5% nonfat dried milk. The membranes were washed three times (10 min per wash) with TBST prior to the incubation for 1 h at room temperature with the anti-topoII antibody (1/2500 dilution in 25 mL of TBST). After three successive washes (10 min with TBST), the membranes were incubated with a goat anti-rabbit antibody conjugated to horseradish peroxidase (Amersham LifeSciences, 1/1000 dilution in 25 mL of TBST) for 30 min while being gently agitated. After four successive washes (10 min each with TBST), the Western blot chemiluminescence reagent from NEN (Boston, MA) was used for the detection. Bands were vizualized by autoradiography.

Cytotoxicity and Cell Cycle Analysis. Cytotoxicity tests were performed as previously described (*14*). For flow cytometry analysis of DNA content, 5×10^5 HL60 cells in exponential growth were treated with 5 μM cryptolepine for 23 h and then washed three times with citrate buffer. The cell pellet was incubated with 125 μL of trypsin-containing citrate buffer for 10 min at room temperature and then with 100 μL of citrate buffer containing a trypsin inhibitor and RNase (10 min) prior to adding 100 μL of propidium iodide at a concentration of 125 μg/mL. Samples were analyzed on a Becton Dickinson FACScan flow cytometer (San Jose, CA) using the LYSYS II software which is also used to determine the percentage of cells in the G1, S, and G2/M phases.

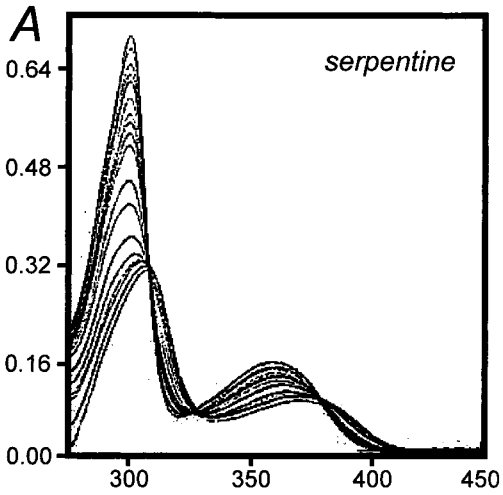

FIGURE 2: Titration of serpentine with calf thymus DNA. The figure contains the absorption spectrum of the free drug and the intermediate and final spectra of the drug−DNA complexes in which the ligand has been sequestered completely by the DNA. To 3 mL of drug solution [20 μM in 1 mM sodium cacodylate buffer (pH 6.5)] were added aliquots of a concentrated DNA solution. Spectra are referenced against DNA solutions of exactly the same molar concentration and were adjusted to a common baseline at 500 nm. The phosphate−DNA/drug ratio increased from 0 to 20 (top to bottom curves at 367 nm).

Detection of DNA Fragmentation. HL-60 cells at a density of about 10^6 cells/mL were treated with various concentrations of cryptolepine for the indicated periods and then collected by centrifugation at 2500*g* for 5 min. The resultant cell pellets were resuspended in PBS buffer containing 5 mM $MgCl_2$ and lysed in 500 μL of TE buffer containing 0.1% SDS and proteinase K (1.5 mg/mL) overnight at 37 °C. After two successive extractions with phenol/chloroform, the DNA was precipitated with ethanol, resuspended in water (100 μL), and treated with RNase A (400 μg/mL) for 2 h at 37 °C. Electrophoresis was performed in 1% agarose gels in Tris-borate buffer.

RESULTS AND DISCUSSION

DNA Binding Affinity

Absorption spectroscopy provides a direct means of estimating the affinity of the drugs for double-stranded DNA. All three drugs exhibit in the near-UV region an absorption band centered at 367 nm. Binding of the drugs to calf thymus DNA induces well-defined bathochromic and hypochromic effects. Results from a typical titration experiment of serpentine with DNA are shown in Figure 2. The two absorption bands centered at 305 and 367 nm are red-shifted by about 10 nm, and the hypochromic effect exceeds 50%. Isosbestic points at 312, 332, and 383 nm can be seen. Similar absorption profiles were recorded with matadine (spectra not shown). The titration experiments were used to determine the apparent association constants for association of the ligands with DNA and the number of sites per

Table 1: Association Constants for Complexes between the Alkaloids and DNA[a]

	K_1	K_2	n_1	n_2
cryptolepine	3×10^6	4×10^4	0.2	0.5
matadine	2.8×10^5	5×10^3	0.2	0.7
serpentine	2.5×10^5	5×10^3	0.16	0.6

[a] Apparent association constants (in M^{-1}) were determined by absorbance titration experiments and Scatchard analyses [in 1 mM sodium cacodylate buffer (pH 6.5)]. The uncertainties in the primary experimental values of K were estimated to be 5−10%.

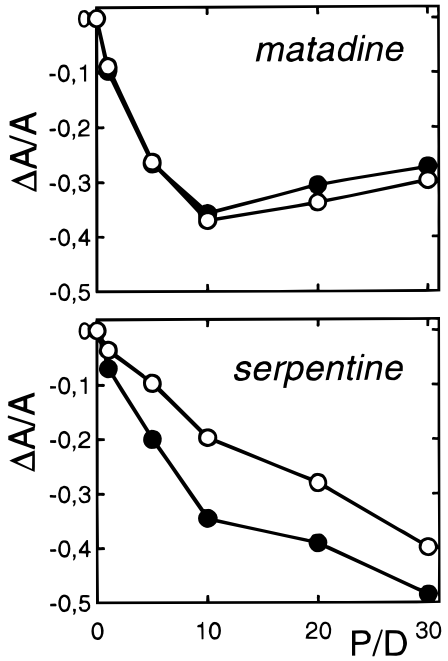

FIGURE 3: Variation of the reduced dichroism ($\Delta A/A$) as a function of the phosphate−DNA/drug ratio (P/D). Electric linear dichroism was recorded at 315 (○) and 380 nm (●) in 1 mM sodium cacodylate buffer (pH 6.5) with an electric field strength of 13 kV. The drug concentration was fixed at 10 μM.

nucleotide n (Table 1). As previously observed for cryptolepine (*14*), the binding curves could not be fitted with the McGhee−von Hippel model for noncooperative binding. Therefore, we resorted to a two-site model (*20*), assuming the existence of two independent noncooperative types of binding, to adjust the experimental data. The binding characteristics for serpentine and matadine are very similar to each other and to the values measured for a related alkaloid 5,6-dihydroflavopereine (*21*). In both cases, the binding affinity is about 1 order of magnitude lower than that of cryptolepine.

Mode of Binding to DNA

Fluorescence Polarization. We recorded the fluorescence polarization spectra for the free drug and drug−DNA complexes at different P/D ratios between 300 and 430 nm so we could calculate the emission anisotropy factor, r. With both drugs, the variations of the anisotropy factor are different at 315 and 380 nm. With serpentine, r decreases with P/D at 315 nm, whereas at 380 nm, it increases with the P/D ratio until a value of about 0.2 is reached (data not shown). This suggests that the orientations of the two transition moments (corresponding to the two absorption bands) are not identical. The situation is slightly different with matadine. In this case, the anisotropy factor remains constant at 315 nm and increases up to 0.2 at 380 nm. The results suggest that the orientation of the pyridoindole chromophore is probably slightly different when matadine and serpentine bind to DNA.

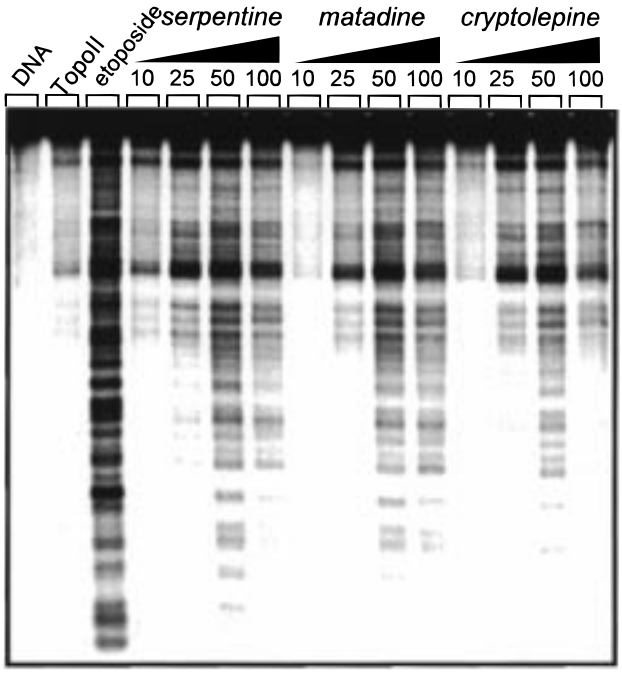

FIGURE 4: Inhibition of topoisomerase II-mediated double-strand cleavage of DNA by the alkaloids. The 5′-end-labeled 9 kbp *Not*I−*Kpn*I restriction fragment from plasmid pMLL (lane labeled DNA) was incubated with purified topoisomerase II in the absence (lane labeled Topo II) or presence of the test drug (micromolar concentration as indicated). Reactions were carried out for 45 min at 37 °C and then stopped with SDS−proteinase K treatment. Double-stranded DNA fragments were analyzed on a 1% alkaline agarose gel containing 0.1% SDS in TBE buffer. Etoposide was used at a concentration of 50 μM.

Electric Linear Dichroism. Differences between matadine and serpentine were observed (Figure 3). With matadine, the reduced dichroism is almost the same at 310 and 380 nm, reaches −0.4 when $P/D = 10$, and then becomes less negative at higher P/D ratios, due to the high concentration of DNA. No plateau is observed with serpentine, and the reduced dichroism is more negative at 380 nm than at 310 nm. The data confirm that the orientations of the two drug chromophores are slightly different upon interaction with DNA. The intensity of the reduced dichroism when the drug is fully bound to DNA ($\Delta A/A = -0.4$ to -0.5) is identical to that measured with the DNA alone at 260 nm in the absence of the ligand ($\Delta A/A = -0.43$). This attests that the drug chromophore is oriented parallel to the DNA base pair planes and strongly suggests that the alkaloids intercalate into DNA.

Topoisomerase II Inhibition

We studied the effect of the plant alkaloids on purified human topoisomerase II using a ^{32}P-labeled *Not*I−*Kpn*I restriction fragment of pMLL as a substrate. DNA cleavage products were analyzed by neutral agarose gel electrophoresis (Figure 4). The three alkaloids promote topoisomerase II-mediated DNA cleavage. The effect is not as pronounced as with the reference topoisomerase II inhibitor etoposide, but

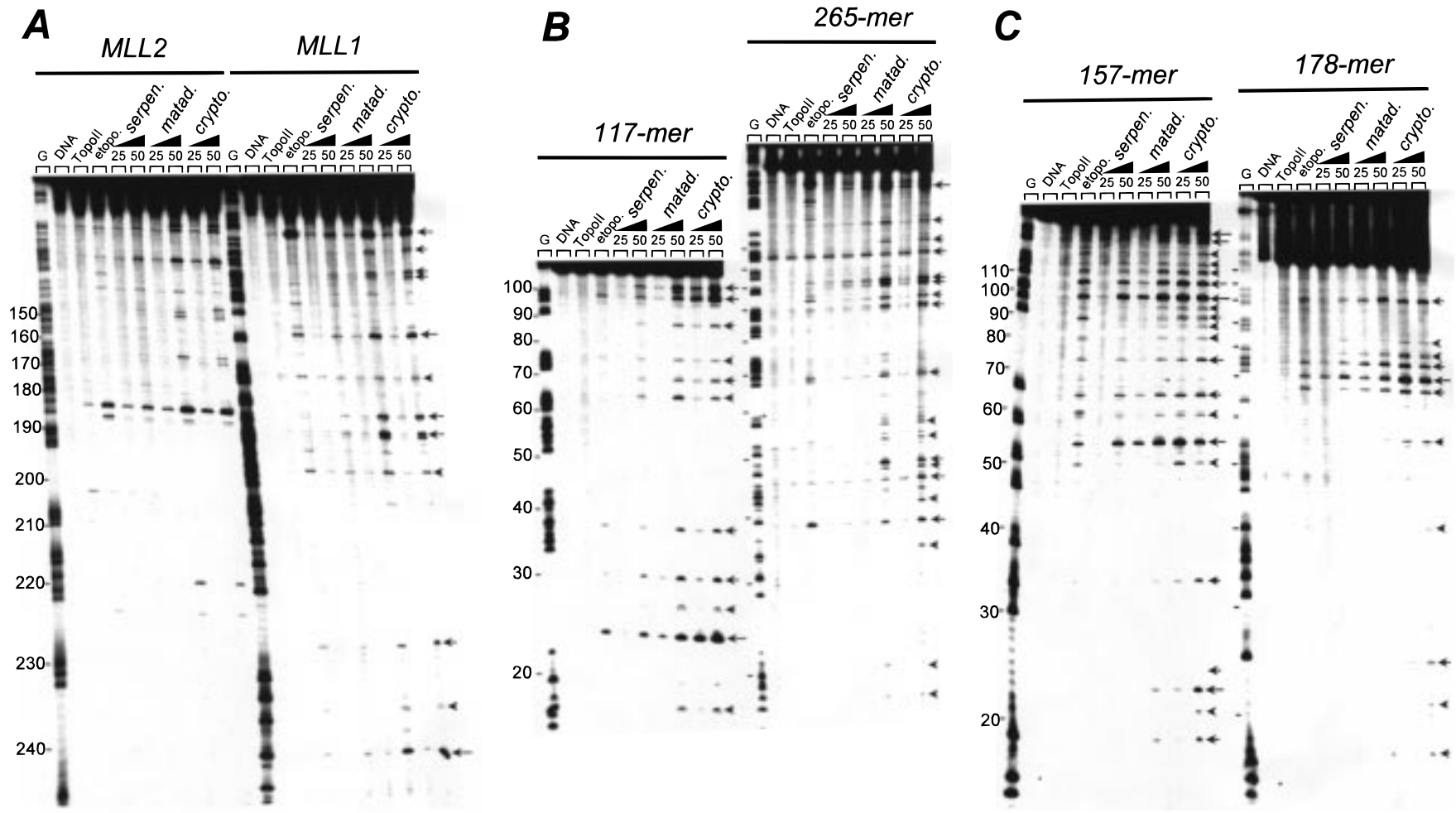

FIGURE 5: Sequence analysis of the cleavage sites stimulated by the alkaloids. Six different restriction fragments were used. In panel A, the two fragments from the plasmid pMLL were obtained by PCR. Panel B shows the results obtained with the *Eco*RI−*Pvu*II fragments from plasmid pBS. In panel C, the fragments were obtained from plasmid pLAZ3 after digestion with *Eco*RI and *Hin*dIII. In each case, the 5′-end-labeled DNA was incubated in the absence (lane labeled Topo II) or presence of the test drug at a concentration of 50 or 100 μM. Etoposide was used at a concentration of 50 μM. Numbers at the side of the gels refer to the nucleotide position of cleavage sites. Drug-stabilized topoisomerase II cleavage sites are denoted by arrows.

a significant level of cleaved DNA fragments can be detected when 50 μM drug is used. The cleavage sites reflect the stabilization of topoisomerase II−DNA covalent (cleavable) complexes. Matadine and serpentine also poison topoisomerase II. The cleavage profiles are very similar, if not identical, for all three alkaloids. This suggests that they induce DNA cleavage by the enzyme at similar sites in the DNA, i.e., that they exhibit the same sequence selectivity. To address this point, a population of topoisomerase II cleavage sites were sequenced. Six 5′-end-labeled restriction fragments were used: the *Eco*RI−*Pvu*II 117 and 265 bp fragments from plasmid pBS, the *Eco*RI−*Hin*dIII 157 and 178 bp fragments from plasmid pLaz3, and two PCR-derived 260 bp fragments from plasmid pMLL (Figure 5). The gels show that cryptolepine is more efficient at inhibiting topoisomerase II than matadine which is itself more effective than serpentine. Cryptolepine stimulates DNA cleavage at numerous sites, whereas only the major cleavage sites can be detected with serpentine. At 50 μM drug, more cleavage sites are detected with cryptolepine than with matadine. Titration experiments revealed that the minimum drug concentration required to inhibit topoisomerase II is lower with cryptolepine than with matadine (10 vs 20 μM).

The cleavage patterns obtained with cryptolepine are slightly different from those observed with etoposide. Although sites common to the two drugs are frequently observed, there are a few cryptolepine-specific sites. For example, on the 265 bp fragment, cleavage occurs at 5′-GCATGC$^{\downarrow}$AAGCTT (position 48) with cryptolepine and matadine but not with etoposide despite the presence of a C on the 3′-side of the cleavage site (position −1). On the MLL1 fragment, three adjacent sites around positions 190 are specific to matadine and cryptolepine: 5′-AAGGG$^{\downarrow}$A$^{\downarrow}$ATGTC$^{\downarrow}$TCGGCC. For a total of 48 cleveage sites localized with accuracy, 18 (37%) are specific to matadine and cryptolepine. The sequences of the cleaved sites were aligned relative to the broken DNA phosphodiester bond, but no clear base preference was detected. The bases on the 3′- and 5′-sides of the cleavage sites can vary, whereas the majority of cutting sites detected with etoposide have a C at position −1 (3′-terminus of the breaks) as expected (*22*). Apparently, the alkaloids do not exhibit a preference for a specific base at the 3′-terminus of the cutting site.

The above experiments indicate that cryptolepine interferes with topoisomerase II in vitro. We then searched to determine if the effect also occurs in cells. For that purpose, we set up an immunoblot assay to identify the drug-stabilized topoisomerase II−DNA complexes in HL60 leukemia cells (Figure 6). In the control samples with no drug, topoisomerase II was found essentially at the top of the CsCl gradient as the free protein. In sharp contrast, with both etoposide and cryptolepine, topoisomerase II was found in the top fractions as well as in fractions 7−10 near the bottom of the gradient where the nucleic acids were localized (as judged from the absorbance measurements at 260 nm). Endogenous topoisomerase II can be trapped onto DNA by cryptolepine in HL60 leukemia cells.

Cytotoxicity and Cryptolepine-Induced Cell Death in HL60 Leukemia Cells

Cryptolepine, but not matadine and serpentine, is toxic to B16 melanoma cells. IC_{50} values of 1.3 and 171 μM were measured with cryptolepine and matadine, respectively. With HL60 leukemia cells, the concentration of cryptolepine required to kill 50% of the cells is 0.8 μM. We searched to determine the mechanism by which cryptolepine kills cancer cells. Most topoisomerase II inhibitors, including etoposide and amsacrine, can induce apoptosis in tumor cells, in particular with leukemia cells (*23*−*26*). HL60 leukemia cells were treated with cryptolepine (1−50 μM) for various periods of time (1 h and up to 24 h). Cell cycle analyses show that a prominent sub-G1 population appears in cryptolepine-treated cells (Figure 7) but only after a long incubation with the alkaloid (23 h). The sub-G1 fraction represents only 3% of cells in the control and reaches 43% upon treatment with the alkaloid. In the same time, the G1 population markedly decreases from 45 to 18%. The sub-G1 population is usually considered apoptotic cells but may also correspond to a necrotic cell population. The biochemical and morphological changes characteristic of apoptosis were examined using two complementary methods: the

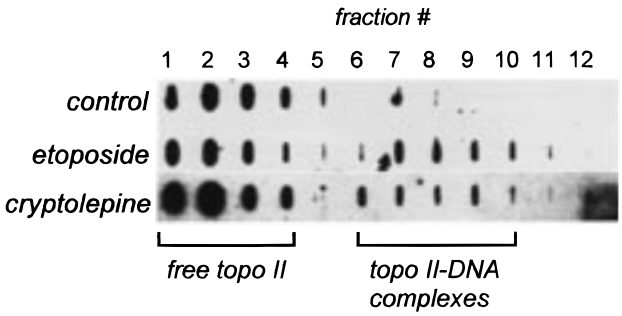

FIGURE 6: Immunoblot analysis of drug-stabilized topoisomerase II−DNA covalent complexes in HL60 murine leukemia cells. Exponentially growing HL60 cells (10^7) were incubated with 50 μM cryptolepine or etoposide for 30 min. The cell lysates were applied to a CsCl gradient and centrifuged overnight. Twelve fractions were collected and analyzed by the slot blot method described in Materials and Methods. Fractions 1−4 contain free topoisomerase II. DNA−topoisomerase II covalent complexes can be detected in fractions 6−10 of the drug-treated samples.

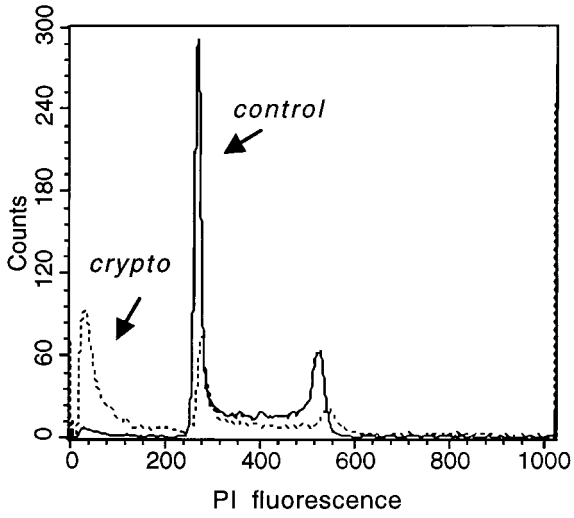

FIGURE 7: Cell cycle analysis of (solid line) untreated and (dashed line) cryptolepine-treated HL60 cells. Cells were incubated with 5 μM cryptolepine for 23 h prior to analysis with the FACScan flow cytometer as described in Materials and Methods. The sub-G1, G1, S, and G2+M populations represent 3, 45, 32, and 19% of the cells in the control and 43, 18, 17, and 10% of the cells in the cryptolepine-treated samples, respectively.

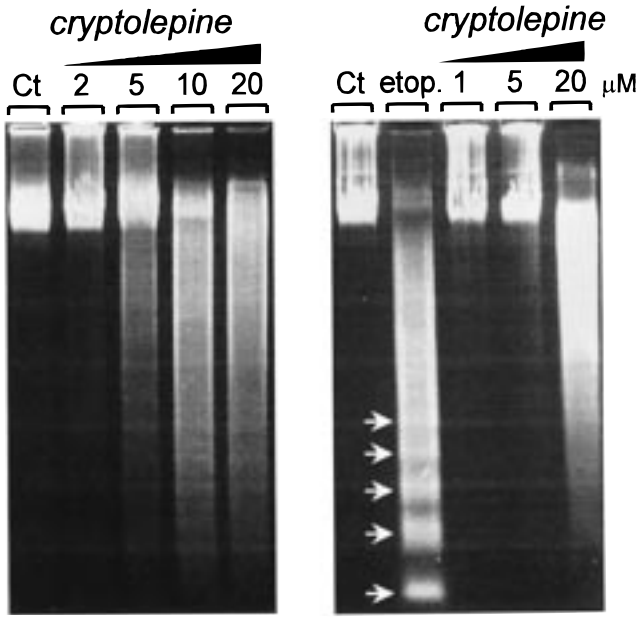

FIGURE 8: Agarose gel electrophoresis of DNA extracted from untreated HL-60 cells (control, Ct) and cells treated with different concentrations (micromolar) of cryptolepine for 15 (left) or 3 h (right). DNA was stained with ethidium bromide after agarose gel electrophoresis. Oligonucleosome-sized DNA fragmentation can be seen in etoposide-treated cells (arrows) but not with cryptolepine.

TUNEL (TdT-mediated dUTP nick end labeling) assay (*27*) and the DNA laddering assay (*28*). No sign of drug-induced apoptosis was detected whatever the cell treatment conditions. Using the TUNEL assay, we did not detect positive (green) cells by fluorescence microscopy (data not shown). The genomic DNA of cryptolepine-treated cells remained intact when using low drug concentrations (<5 μM). At higher concentrations (up to 20 μM), the genomic material becomes degraded but there was no internucleosomal cleavage (Figure 8). In the control experiments performed with etoposide, a clear pattern of DNA internucleosomal fragmentation was observed. The TUNEL and DNA laddering assays concur that cryptolepine does not induce apoptosis in HL60 cells. Cells treated with cryptolepine probably die via necrosis.

CONCLUSION

As mentioned in the introductory section, cryptolepine, matadine, and serpentine have been used for a long time in African folk medicine in the form of plant extracts. So far, nothing was known concerning their potential intracellular targets and mechanism of action. Our study suggests that DNA and topoisomerase II are two potential targets for the drugs in cells. The alkaloids behave as typical DNA-intercalating agents, but their affinities for double-stranded DNA vary significantly. Cryptolepine, the simplest of the three alkaloids, binds relatively tightly to DNA, whereas matadine and serpentine, which have a more complex structure, exhibit a 10-fold reduced affinity for DNA. With the latter anhydronium alkaloids, the presence of a bulky side chain appended to the pyridoindole chromophore must hinder the access of the drug to intercalation sites in DNA.

The demonstration that the three alkaloids are topoisomerase II poisons may have important implications in terms of drug design. It will be interesting to evaluate the anti-topoisomerase II activity of cryptolepine analogues, including the analogues which are being developed as anti-hyperglycemic compounds (*3*, *4*). One might also plan to develop synthetic analogues targeting topoisomerase II as antitumor drugs. In addition, it will be important to determine whether related alkaloids such as strychnoxanthine, melinonine, and dihydroflavopereine can also interfere with topoisomerase II functions. This would be particularly interesting with alstonine, an inactive isomer of serpentine. These alkaloids may also poison other types of topoisomerase II such as the topoisomerase II from plasmodium species, thereby suggesting a possible mechanism of antimalarial activity. Clearly, this study opens a number of doors and sets the stage for subsequent investigations.

ACKNOWLEDGMENT

C.B. thanks Brigitte Baldeyrou, Nicole Wattez, and Christine Mayeu for expert technical assistance and the Service Commun d'Imagerie Cellulaire de l'IFR22 for access to the fluorescence microscope.

REFERENCES

1. Pezzuto, J. M. (1997) *Biochem. Pharmacol. 53*, 121−133.
2. Clinquart, E. (1929) *Bull. Acad. R. Med. Belg. 9*, 627−635.
3. Bierer, D. E., Dubenko, L. G., Zhang, P., Lu, Q., Imbach, P. A., Garofalo, A. W., Phuan, P.-W., Fort, D. M., Litvak, J., Gerber, R. E., Sloan, B., Cooper, R., and Reaven, G. M. (1998) *J. Med. Chem. 41*, 2754−2764.
4. Bierer, D. E., Fort, D. M., Mendez, C. D., Luo, J., Imbach, P. A., Dubenko, L. G., Gerber, R. E., Litvak, J., Lu, Q., Zhang, P., Reed, M. J., Waldeck, N., Bruening, R. C., Noamesi, B. K., Hector, R., Carlson, T. J., and King, S. R. (1998) *J. Med. Chem. 41*, 894−901.
5. Luo, J., Fort, D. M., Carlson, T. J., Noamesi, B. K., nii-Amon-Kotei, D., King, S. R., Tsai, J., Quan, J., Hobensack, C., Lapresca, P., Waldeck, N., Mendez, C. D., Jolad, S. D., Bierer, D. E., and Reaven, G. M. (1998) *Diabetic Med. 15*, 367−374.
6. Kirby, G. C., Noamese, B. K., Paine, A., Warhurst, D. C., and Phillipson, J. D. (1995) *Phytother. Res. 9*, 359−363.
7. Boye, G. L., and Oku-Ampofo (1983) in *Proceedings of the First International Seminar on Cryptolepine*, July 27−30, 1983, pp 37−40, University of Science and Technology, Kumasi, Ghana.
8. Wright, C. W., Phillipson, J. D., Awe, S. O., Kirby, G. C., Warhurst, D. C., Quetin-Leclercq, J., and Angenot, L. (1996) *Phytother. Res. 10*, 361−363.
9. Bonjean, K., De Pauw-Gillet, M.-C., Defresne, M.-P., Colson, P., Houssier, C., Dassonneville, L., Bailly, C., Wright, C., Quetin-Leclercq, J., and Angenot, L. (1997) *Anticancer Res. 17*, 4068−4069.
10. Quetin-Leclercq, J., Coucke, P., Delaude, C., Warin, R., Bassleer, R., and Angenot, L. (1991) *Phytotherapy 30*, 1697−1700.
11. Wright, C. W., Allen, D., Phillipson, J. D., et al. (1993) *J. Ethnopharmacol. 40*, 41−45.
12. Beljanski, M., and Beljanski, M. S. (1986) *Oncology 43*, 198−203.
13. Beljanski, M., and Beljanski, M. S. (1982) *Exp. Cell. Biol. 50*, 79−87.
14. Bonjean, K., De Pauw-Gillet, M.-C., Defresne, M.-P., Colson, P., Houssier, C., Dassonneville, L., Bailly, C., Greimers, R., Wright, C., Quetin-Leclercq, J., Tits, M., and Angenot, L. (1998) *Biochemistry 37*, 5136−5146.
15. Houssier, C., and O'Konski, C. T. (1981) in *Molecular Electro-Optics* (Krause, S., Ed.) pp 309−339, Plenum Publishing Corp., New York.
16. Houssier, C. (1981) in *Molecular Electro-Optics* (Krause, S., Ed.) pp 363−398, Plenum Publishing Corp., New York.

17. Bailly, C., Hénichart, J.-P., Colson, P., and Houssier, C. (1992) *J. Mol. Recognit. 5*, 155−171.
18. Colson, P., Bailly, C., and Houssier, C. (1996) *Biophys. Chem. 58*, 125−140.
19. Kerckaert, J.-P., Deweindt, C., Tilly, H., Quief, S., Lecocq, G., and Bastard, C. (1993) *Nat. Genet. 5*, 66−70.
20. Cantor, C. R., and Schimmel, P. R (1980) *Biophysical Chemistry*, W. H. Freeman and Co., San Francisco.
21. Caprasse, M., and Houssier, C. (1983) *Biochimie 65*, 157−167.
22. Pommier, Y., Capranico, G., Orr, A., and Kohn, K. W (1991) *Nucleic Acids Res. 19*, 5973−5980.
23. Barry, M. A., Reynolds, J. E., and Eastman, A. (1993) *Cancer Res. 53*, 2349−2357.
24. Bertrand, R., Solary, E., Jenkins, J., and Pommier, Y. (1993) *Exp. Cell Res. 207*, 388−397.
25. Walker, P. R., Smith, C., Youdale, T., Leblanc, J., Whitfield, J. F., and Sikorska, M. (1991) *Cancer Res. 51*, 1078−1085.
26. Solary, E., Bertrand, R., Kohn, K. W., and Pommier, Y. (1993) *Blood 81*, 1359−1368.
27. Ben-Sasson, S. A., Sherman, Y., and Gavrieli, Y. (1995) *Methods Cell Biol. 46*, 29−39.
28. Compton, M. M. (1992) *Cancer Metastasis Rev. 11*, 105−119.

BI990094T